THE JOURNAL OF PHYSICAL CHEMISTRY A

ARTICLE

pubs.acs.org/JPCA

Maximum Probability Domains in Crystals: The Rock-Salt Structure

Mauro Causà*,† and Andreas Savin*,‡

†Dipartimento di Chimica Paolo Corradini, Universitá degli Studi di Napoli "Federico II", Via Cintia, 80126 Napoli, Italy

‡Laboratoire de Chimie Théorique, CNRS and UPMC Univ Paris 6, 4 place Jussieu, 75252 Paris, France

Supporting Information

ABSTRACT: The present paper studies MX crystals in rock-salt structure (M: Li, Na, K; X: F, Cl, Br, I). They are often described as being formed by ions. Pictures based on quantum mechanical calculations sustain and quantify it. The tools used are (i) the Quantum Theory of Atoms in Molecules, (ii) the Electron Localization Function, and (iii) the maximization of the probability to find in a spatial domain a number of electrons equal to that of the ion under consideration. The present paper shows that the images provided by these three different tools to analyze the quantum mechanical calculations yield, for these systems, very similar results, in the sense that the spatial domains and probability distributions are close. While results for the first two methods are already present in the literature, the last of the methods is applied for the first time to these systems, and details about the method of calculation and program are also given.

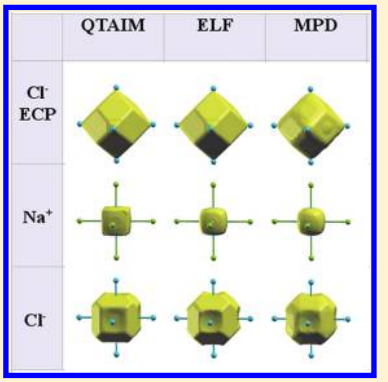

I. INTRODUCTION

By firmly grounding a tool to analyze chemical bonding, the Quantum Theory of Atoms in Molecules (QTAIM),[1] Prof. Richard F. W. Bader also stimulated the interest of researchers to provide new tools to understand chemistry. Among them are the Electron Localization Function of Becke and Edgecombe[2] and the Maximum Probability Domains (MPDs).[3] These three methods are used below to analyze results of quantum mechanical calculations (at Hartree−Fock level) for crystals in rock-salt structure (MX, M: Li, Na, or K; X: F, Cl, Br, or I). Results obtained for QTAIM and ELF (and one of the forms of a closely related electron localizability indicator, ELI-D[4]) were already published.[5−11]

In this paper, we analyze maximum probability domains (MPD), the regions of space that maximize the probability to find in them a given number of electrons in them.

Although MPDs are based on a clear and simple quantum mechanical concept, it is not self-evident that chemical concepts can be derived from them. At the present stage, we have to learn how MPDs work. We present in this paper, results for relatively simple crystals in rock-salt structure.

Because the calculations were performed using a recently developed program for crystals, a few details about the implementation are present, too.

The paper is structured as follows. First we define the MPDs, recall their main features, and make a short comparison to other related methods. Next, we give some details about our calculation, in particular, the way MPDs are obtained. In the Results section, we notice the similarity of the shapes of the MPD ions to those obtained with QTAIM or ELF, and interpret their shapes and also the changes in the ionic volumes that we relate to changes of the counterion and of the Madelung forces. We also look at the probabilities to find a given number of electrons in the spatial domains. We find a relatively high probability to find as many electrons as in the formal ions. We also find, however, some probability to find more or less electrons than in the formal ions. When discuss the possibility to define charges not based upon the average number of electrons in the domains, but also based upon the probability distribution. We further notice that the often presented indicators, mean and variance, can lead to inaccurate descriptions of the probability distribution. Some Supporting Information is given in the appendices (simple systems, interpretation of the density and charges). Furthermore, the numerical data on which we base our discussion can be found online, as Supporting Information.

II. DEFINITIONS

A. Objective and Choices. *1. Electron Number.* We would like to identify spatial subsystems in a given electronic system by specifying a given electron number, ν. This is done, for example, when searching for atomic shells, the electron pairs of the Lewis model, and so on. An essential point of the approach we take is to let ν be a freely chosen parameter. For example, one would chose $\nu = 2$ when trying to find a Lewis electron pair from quantum mechanical calculations. In the present paper, we search for the

Special Issue: Richard F. W. Bader Festschrift

Received: June 15, 2011
Revised: August 25, 2011
Published: September 29, 2011

ions in crystals in the rock-salt structure, and choose $\nu = 2$ for finding the Li^+ ion, $\nu = 10$, for finding the F^- ion, and so on. Thus, we consider the positive integer ν defined by the question the user asks.

2. Spatial Region. The next choice to be made is for defining a spatial region, Ω. To not impose external requirements, we choose the spatial region to have sharp boundaries: a point in space either belongs to Ω or does not. In contrast to basins, as used in QTAIM or ELF, we allow the MPDs to be spatially disconnected.

Quantum mechanics tells us that, for a given state Ψ, finding a given number of electrons ν in Ω is only possible with a certain probability, p. We have, thus, to see our subsystem as an open system, able to exchange electrons with the region outside Ω, analogously to QTAIM density basins.

B. Maximum Probability Domains. *1. Definition.* We are now in a position to define the maximum probability domains (MPDs) as the regions of space for which the probability to find ν electrons is maximal. To be more precise, let us consider an electronic system described by a wave function Ψ. The probability to find ν and only ν electrons out of N in a three-dimensional region Ω is given by

$$p_\nu(\Omega) = \binom{N}{\nu} \int_\Omega dx_1, ..., dx_\nu \int_{\bar{\Omega}} dx_{\nu+1}, ..., dx_N |\Psi(x_1, ..., x_N)|^2 \quad (1)$$

where $\bar{\Omega}$ is the remaining part of the three-dimensional space, R^3/Ω, and the binomial coefficient is needed for taking into account the permutations of the electrons. For a given ν, the region Ω for which $p_\nu(\Omega)$ is maximal, the MPD, depends on ν, and is written as Ω_ν.

The definition in eq 1 can be immediately extended to ensembles.

Please notice that p_ν is not a reduced ν-particle density integrated over the domain Ω. In the latter, the integration over $\nu + 1$, ..., is performed over the whole space, and not over R^3/Ω. An example of the difference between the two definitions is discussed in Appendix A, showing that the integral of the one-particle density yields the average number of electrons in Ω and not the probability to find one electron in Ω.

2. Physical Multiplicity. As a rule, several solutions exist to the optimization of Ω for given ν, Ω_ν. This is physically motivated. For example, in the NaF crystal, we may expect one Ω_{10} corresponding to the Na^+ ion, and another Ω_{10} that corresponds to the F^- ion. Furthermore, several symmetry equivalent Ω_νs can exist. In the NaF crystal, for instance, if one Ω_{10} is found and associated to one of the Na^+ ions, there are infinitely many such Ω_{10} produced by translational symmetry that can be associated to the other Na^+ ions of the crystal. Symmetry can also produce less trivial situations. For example, in the bent Si_2H_2 molecule, we find two sets of three Ω_2s, one arranged as an "upward" oriented triangle, the other as a "downward" oriented triangle (see Figure 18 of ref 12). These solutions are equivalent, as the nuclear arrangement is invariant to inversion, but not the "triple pair" structure. This feature corresponds to one known for localized orbitals, is related to resonanting structures and did not show up in the present study.

C. Synthetic Information. *1. Mean.* One may provide compact information by using some significant numbers. The mean, or average number of electrons in Ω is given by

$$\mu(\Omega) = \sum_{\nu=0}^{N} \nu p_\nu(\Omega) \quad (2)$$

It can be also obtained by integrating the density electron $\rho(r)$ over the domain Ω and is, thus, the population of Ω. To see it, we can write

$$\int_\Omega \rho(r) d^3r = \int_\Omega \langle\Psi|\hat{\rho}(r)|\Psi\rangle d^3r = \langle\Psi| \int_\Omega \hat{\rho}(r) d^3r |\Psi\rangle \quad (3)$$

where we introduced the density operator, $\hat{\rho}(r) = \Sigma_{i=1}^{N} \delta(r - r_i)$. We write

$$\int_\Omega \hat{\rho}(r) = \sum_{i=1}^{N} \theta_\Omega(r - r_i) = \hat{N}_\Omega(r) \quad (4)$$

where $\theta_\Omega(r - r_i)$ is 1 when electron i is in Ω and 0 when it is outside it.[13] $\hat{N}_\Omega$ counts the electrons in Ω. The expectation value of $\hat{N}_\Omega$, $\langle\Psi|\hat{N}_\Omega|\Psi\rangle$, yields the average number of electrons in Ω. However, expectation values can be also written as in eq 2 (see, e.g., chapter III.C.4 of ref 14). The implication of this viewpoint on the physical interpretation of the electron density is discussed in Appendix A.

In some situations, when the domain Ω contains a nucleus, one can prefer to replace μ by a charge, defined as the difference between the nuclear charge and the population, $\mu(\Omega)$.

2. Unphysical Multiplicity of Domains Defined by Means. The multiplicity of MPDs should not be confused with that arising from unphysical requirements. For example, one might think of defining Ω such that the integral of the electron density over Ω yields the integer number ν ($0 < \nu < N$). For the latter definition, there are infinitely many Ωs satisfying the required condition. For example, define in the Be atom a sphere, centered on the nucleus, with radius R. Let R_c be the radius of the sphere such that the integral over the density in this sphere is exactly equal to two. For any radius $R_1 < R_c$, there is a radius $R_2 > R_c$ such that the integral of the density over the spherical shell defined by R_1 and R_2 yields the same value, two. This is not the case for the MPDs, compare Figure 7 in ref 15. This difference can be understood by the fact that integrating the density yields the average value $\mu(\Omega)$ that can be achieved with several distributions, $p_0(\Omega)$,$p_1(\Omega)$, ..., $p_N(\Omega)$.

3. Variance. Another synthetic information about the probability distribution, $p_0(\Omega)$,$p_1(\Omega)$, ..., $p_N(\Omega)$ is given by the variance,

$$\sigma(\Omega)^2 = \sum_{\nu=0}^{N} [\nu - \mu(\Omega)]^2 p_\nu(\Omega) \quad (5)$$

The population and variance can be found in literature for discussing spatial domains (see, e.g., refs 11 and 16−18). Variance can be valuable, as the average, μ, does not necessarily reflect the probability distribution. For example, let us consider the dissociated hydrogen molecule and choose Ω on one side of the plane that is perpendicular to the line connecting the nuclei, and is equally distant from the two nuclei. For the ground state,

we have $p_1(\Omega) = 1$ and $p_0(\Omega) = p_2(\Omega) = 0$, while for the ionic resonant state, $H^+\cdots H^- \leftrightarrow H^-\cdots H^+$, we have $p_1(\Omega) = 0$ and $p_0(\Omega) = p_2(\Omega) = 1/2$. For both cases, $\mu = 1$, while the variance is different (0 in the former, 1 in the latter case).

4. Insufficient Information from Synthetic Indicators. Of course, by using the synthetic indicators, μ, σ^2, some information gets lost; in general, a simple counting shows that there is more information in p_0, p_1, ..., p_N, $\Sigma_\nu p_\nu = 1$ than in just two numbers. One can ask, however, what happens if all probabilities are close to 0, except $p_{\nu-1}$, p_ν, and $p_{\nu+1}$. Are μ and σ^2 sufficient? A numerical example, based on the data obtained, shows that μ and σ^2 do not accurately reconstruct $p_{\nu-1}$, p_ν and $p_{\nu+1}$ although the premise of having the other probabilities small seems to be satisfied. It will be presented in the Results section.

5. Fluctuations. Electrons are free to cross the sharp boundaries we have defined. Let us imagine for a didactical purpose a time-dependent picture. First, let us imagine that all ν electrons are in Ω_ν. To get to the physical probability distribution, we imagine now that electrons cross the surface of Ω_ν. As electrons get in or out Ω_ν, the probability to find ν and only ν electrons in Ω_ν decreases, while that of finding $\nu + 1$ or that of finding $\nu - 1$ in this spatial region increases. At the same time, the variance is increased. A change of the average number of electrons does not necessarily take place. When an electron quits a domain Ω_ν, and enters another one, equivalent to the first, we at the same time increase the probability to find $\nu + 1$ and that to find $\nu - 1$ electrons. (With the definition of p_ν, eq 1, we treat only one domain at a time.) However, when the two domains are of different nature, a bias between the directions of surface crossing exists, and the average number of electrons is affected. (Of course, the process can be more complicated than the one just described, which considered only ν and $\nu \pm 1$ electrons in Ω, but this should be sufficient for a qualitative discussion.)

To pin down some factors influencing the surface crossing, a simple model for two closed shells at variable distance, and varying degree of compactness is given in Appendix B. It confirms the intuitive picture that as distance (R) times compactness (ζ) increases, the probability of surface crossings decreases.

We can further expect that surface crossings are more frequent when the contact with other domains is increased. For example, for independent particles in a box, the exchanges are less important when Ω_2 is at one of the ends of the box, than for Ω_2 in the center of the box.

6. Alternative Charges. Analyzing probabilities opens a different perspective on viewing charges. While the classical one is based on the average electron number in a domain, one can instead present the probability to find different electron numbers in the same domain. To illustrate the difference let us take two simple examples. The first one is the already mentioned case of the symmetrically divided dissociated H_2 molecule, in the ionic resonant state: the subsystems are charged, but the average charge is zero. Another example is that of the dissociated H_2^+ molecule, $H^+\cdots H \leftrightarrow H\cdots H^+$, with the space divided in two halves, as for the dissociated H_2 molecule. The charge of one of the hydrogen atoms is 1/2, although we could alternatively see it as a statistical mixture of neutral H atoms and ions.

7. Probabilities for Independent Particles. It is possible to obtain some Ω_ν in situations that are not physically significant. It has been proposed[19] to consider statistically independent particles as a reference. In this situation, the probability to find ν particles out of N is given by the binomial distribution,

$$p_\nu^{\text{ind}} = \binom{N}{\nu} b^\nu (1-b)^{N-\nu} \tag{6}$$

$b \in (0, 1)$ is a parameter of the distribution, and is related to the mean of this distribution, bN. We can choose b to maximize p_ν^{ind} for a selected ν, λ. This yields $b = \lambda/N$. In this paper, we are interested in crystals, so let us take N to infinity. We now obtain the Poisson distribution, $p_\nu^{\text{ind}} \rightarrow \exp(-\lambda)\lambda^\nu/\nu!$. For the ions we discuss $\lambda \geq 2$, and the largest probability for independent particles is thus smaller than $2\exp(-2) \approx 0.27$. We obtained for the ions in the rock-crystal structure much larger values for the probabilities. This is due to the fact that the electrons are not independent, even when described with a Hartree−Fock wave function. For the latter, the Pauli principle is acting, and this is reflected in the calculated probabilities.

D. Comparison of MPDs with Other Spatial Domains. *1. Objects Studied.* An important difference between MPDs, on one side, and QTAIM or ELF, on the other side, is the object of study. In the QTAIM the density basins correspond to "atoms". Of course, these "atoms" can be closer to "ions", as they are in the crystals studied in this paper. For ELF, one mostly searches for bonds or lone pairs and not for atoms;[2] the basins are mostly (but not always) attributed to pairs of electrons.[20] Exceptions are present when dictated by symmetry, for example, for atomic shells, as ELF sometimes produces averages of pictures, for example, the L shell of the Ne atom, can be seen as a smeared picture of the four valence electron pairs. One can deliberately join different ELF basins to a single domain, especially when one thinks that the basins are not well separated and remind of a chemical concept, such as an atomic shell, see, for example, refs 20−22. For the present paper, collections of ELF basins were always chosen to be attributed to a given ion. As stated in the section defining MPDs, for these, the user is in charge of defining the case to study, that is, to chose a given ν (the optimization defining Ω_ν). We like to see this as a supplementary freedom existing with MPDs, allowing the user to ask several questions. Please notice that MPDs are physically defined from the start by a physical construct, and not by using a mathematical construct, for example, a basin of a function, even if this function has a clear physical meaning.

The mentioned differences do not imply that in specific cases the results with the QTAIM, ELF, or MPDs are not similar. On the contrary, the ionic domains presented in this paper are similar for QTAIM, ELF, and MPDs.

2. MPDs Do Not Partition Space, but Basins Do. Because each of the Ω_νs is optimized separately, their collection does not necessarily provide a partition of space: the MPDs can leave out portions of space, or overlap. In practice, it is observed that for most cases studied up to now, such a partition is roughly, but not exactly, achieved. Up to now, there is no general proof, but we have some analytical results, for simple models, showing this explicitly.[23] There are also numerical examples where Ω_νs do overlap. It is not clear yet whether these are desirable features or not. At the present stage, we find the lack of partitioning an interesting feature, worth to be explored. Empty regions of space show up, for example, in the diamond structure in the regions corresponding to the "holes".[24] Overlapping regions show up in unstable cases, such as transition states.[12] This non-partitioning of space is to be contrasted to the description given not only by

QTAIM and ELF where basins divide space, but also by loges, to be discussed below.

3. MPDs Are Not Loges. The method of MPDs reminds of the method of loges of Daudel and co-workers.[25−27] There, one defines a partition of space into M regions, called loges, and (in the later variants) minimizes the missing information function,

$$H(x_1, ..., x_M) = -\sum_k P(x_k) \log_2 P(x_k) \quad (7)$$

where x_k is a given distribution of electrons into the loges and P its probability. To obtain MPDs one only optimizes one domain at a time. Here are some reasons for preferring MPDs to a partition into loges:

- It is more difficult to optimize a partition of the space than to optimize a given spatial domain.
- When optimizing a partition of space, some uninteresting situations can be favored, for example, having no electrons in some vanishingly small loge (one is certain of finding no electron in a vanishingly small region of space[23]).
- Partitioning the whole space is often not needed, as one is generally only interested in describing a specific region of space (e.g., a given bond, the active site of the protein, etc.).
- Partitioning needs a good treatment of all loges. If one of the regions is badly described, for example, because starting from a wrong prejudice, it may affect the final result everywhere, even if the error was produced in the part of space, which is considered irrelevant for the problem studied.
- In a very large system, the probability of having a distribution, x_1, corresponding to "the chemical (Lewis) arrangement" becomes vanishingly small. Even if the probability that the number of electrons ν in a given loge is large (but <1), when there are many loges, we can be almost sure that the number of electrons is different from ν in one of the many equivalent loges.

III. PROGRAM IMPLEMENTATION

A. Obtaining the Domains. *1. Ω on a Grid.* The algorithm used in the program is now described. A simplified, schematic description is presented in Figure 1.

To obtain the MPDs, first a regular cubic grid, G, is generated. Typically, the spacing of the grid points is 0.05 bohr. Subsets of the set of grid points, $D \subseteq G$, are selected; all points in D are considered to be inside a spatial domain that can be an atomic or ELF basin, or the domain Ω to be optimized to yield the MPD. To approximate the surface of a spatial domain, a subset of points of is chosen, $S \subseteq D$; all points in S have less than six neighbor grid points. The surface S is triangulized by choosing the vertices of the triangles from the nearest neighbors in S.

2. Optimizing Ω A first guess for the MPD can be an atomic or ELF basin, defined on a grid, or another domain, chosen by the user (a sphere, an ellipsoid, a cube, or a previously obtained MPD). For optimization, the barycenter of the triangles (of the surface S) are moved along the normals. The displacements are proportional to the shape derivatives computed at the barycenter;[15] they are larger at the start of the optimization, smaller toward the end.

During the optimization process, certain regions of Ω can collapse to a surface or even points. These low-coordinated grid points are eliminated both from Ω and S.

B. Obtaining the Probabilities. *1. Formula.* The computation of $p_\nu(\Omega)$, eq 1, is less difficult as it may seem, at least for certain forms of the wave function. In particular, for a single Slater determinant, as it is produced by Hartree−Fock or Kohn−Sham calculations, one first computes the overlaps of all occupied orbitals over the regions Ω,

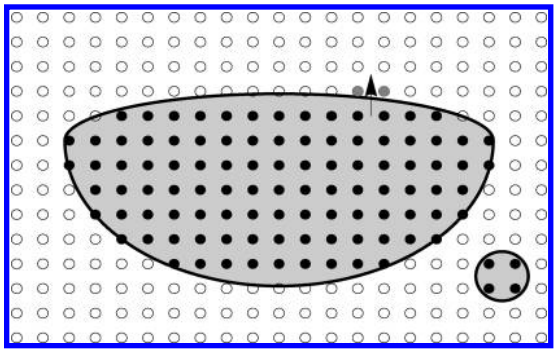

Figure 1. Schematic, 2D representation is shown, to explain the algorithm used. The grid points, belong to the set G, are shown as empty or filled circles. The domain Ω is shaded. The grid points selected to describe Ω belong to the set D, are shown as full black circles. The shape derivative, computed at the origin of the arrow, indicates that Ω has to be extended in the direction shown by the arrow. In the next step, the gray shaded circles will be made part of D. This operation is repeated for all pairs of neighboring grid points close to the border of D. During optimization, the subdomain may not only change size and shape, but also merge, or one of them may disappear.

$$S_{ij}(\Omega) = \int_\Omega \phi_i(x)\phi_j(x)dx \quad (8)$$

Such integrals are also used when computing the variance in atomic or ELF basins.[11,16−18] Next, the eigenvalues of the matrix with elements S_{ij} are obtained. From them, the probabilities are quickly computed for all ν, with the Cancès recursive formula.[15]

The effect of correlation is not explored in this paper. For correlated wave functions, the computation of $p_\nu(\Omega)$ is possible, too, for example, with multideterminant wave functions,[28,29] or even for more complicated forms, by using Quantum Monte Carlo.[12,30]

2. Numerical Implementation. To obtain the overlap integrals S_Ω, eq 8, needed for computing the probabilities, the integrand is decomposed into local contributions, as proposed by Boys and Rajagopal,[31] and extensively used in density functional calculations (see, e.g., refs 32−34),

$$S_{ij}(\Omega) \approx \sum_k \phi_i(x_k)\phi_j(x_k)w_k f(x_k) \quad (9)$$

The quadrature points x_k and weights w_k are the ones used by Becke.[32] The crystal orbitals used are Wannier localized.[35]

The partitioning function, $f(x)$, is close to one if x is inside Ω and close to zero otherwise. We use for $f(x)$ the form of a Fermi-Dirac distribution function, $f(x) = 1/\{1 + \exp[\beta(x_k - b_k) \times n_k]\}$, where n_k is the surface normal in b_k, the triangle barycenter closest to the quadrature point x_k. It was found convenient to choose $\beta = 50$. Numerical tests show that the accuracy achieved is around 1%.

C. Further Information. *1. Volume of Ω;* The volume of Ω can be approximated by the integration scheme used for $S_{ij}(\Omega)$, replacing ϕ_i and ϕ_j in eq 9 by unity.

2. QTAIM/ELF Branch of the Program. To obtain the basins (for QTAIM or ELF), the attractors (maxima) of the corresponding function are found by searching them first on the grid and by later refining the search by using analytical gradients.

All the points on the regular cubic grid leading to a given maximum (by using analytical gradients) form our representation of the basin.

The algorithms in this branch of the program differs presently from that used for MPDs. The volumes of the basins are approximated by the number of points inside the domain times the "volume element", defined by the third power of the smallest distance between two grid points. For obtaining the overlap integrals, a strict cutoff is used in eq 9 for $f(x)$, $\beta \rightarrow \infty$.

IV. TECHNICAL DETAILS

A. Basis Functions and Pseudopotentials. Single-determinant (Hartree−Fock) wave functions are produced with the CRYSTAL program.[36−39] The experimental crystal structures were used.[40,41] For Br and I, small core pseudopotentials were used.[42−44] For some of the calculations, alkali metal pseudopotentials were used, too.[45] The basis sets were of valence triple-ζ plus polarization quality, mostly taken from the CRYSTAL basis data sets. They were taken from ref 46 for Li, with a d function added, with exponent 0.6; from ref 47 for Na; from ref 48 for K; from ref 49 with one d function added, with exponent 0.8, for F; and from ref 50 with one d function added, with exponent 0.5, for Cl. As the CRYSTAL database does not contain basis sets for Br and I with small core pseudopotentials, new basis sets were generated for this case. They are given in a Supporting Information file.

B. Plots. The domains are plotted using the program Xcrysden.[51,52] The other graphs are produced with Mathematica.[53]

V. RESULTS

A. Shapes and Sizes. *1. Similarity between QTAIM, ELF, and MPD Domains.* As, by the definition of the MPDs, the spatial domains are generated to maximize the probability to find in it as many electrons as in the free ion, we assign this region to cations, or anions, and not to neutral atoms. In this sense, the MPDs are the best regions for describing ions in a crystal. For atomic or ELF domains, the definition did not explicitly request the generation of domains defining ions. It turns out, that the spatial domains for the ions in the crystals MX (M: Li, Na, K; X: F, Cl, Br, I) in rock-salt structure are quite similar when obtained with the three approaches considered for this paper, as can be seen in Figure 2 which shows, for NaCl, left to right column, the domains obtained with QTAIM, ELF, or MPDs, respectively.

2. Exclusion. To understand the shape of these domains let us first consider those produced using pseudopotentials (effective core potentials, ECPs) for the alkali metal atoms, so that only halogens are explicitly present. In this case, the domains correspond to Wigner-Seitz (Voronoi) cells obtained for the sublattice of the halogens, Figure 2, top row. In all-electron calculations, cations claim a region around the alkali metal nucleus (cf., Figure 2, middle row). For hard cations, the attributed region should have a nearly spherical shape. For cations as soft as the anions, we intuitively expect planes perpendicular to the cation−anion line to define the separation surface. We see (Figure 2, middle row) that the shape is, in general, in-between these extreme situations, as noted previously in the literature, see, for example, refs 5 and 11. The anions suffer from the exclusion effect of the cations, and the remaining part of the space provides the somewhat peculiar shapes for the anions X^-, Figure 2, bottom row.

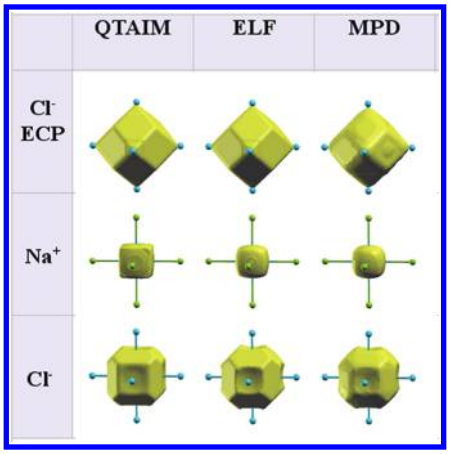

Figure 2. Domains in the NaCl crystal, as obtained from QTAIM, ELF, and MPDs (columns, left to right), when cations are replaced by effective core potentials (i.e., Wigner-Seitz cells for the anion sublattice), for the cation, and for the anion (rows, top to bottom).

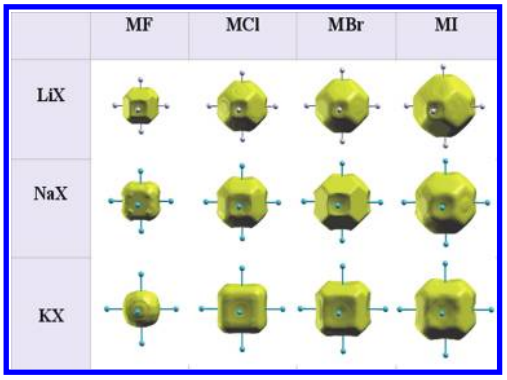

Figure 3. MPDs for the X^- anions in MX crystals, for M: Li to K (rows, top to bottom), and X: F to I (columns, left to right).

3. Relative Sizes Affect Shapes. The relative size of the ions also affects the shapes. As one can expect, the size of the cations increases from Li^+ to K^+, and that of the anions from F^- to I^-, compare Figure 3, and changing the size of the cation affects the shape of the anion. For the small Li^+ in LiI, the shape of the domains of the anions looks almost like that of the halogen sublattice Wigner-Seitz cells, while for the larger K^+ in KCl, both ionic domain are closer to having a cubical shape.

It is interesting to notice that with MPDs the domain of F^- in KF does not seem to be in contact with that of the neighboring F^-. With the QTAIM and ELF domains, it seems that both the domains for K^+ and F^- have cubical shapes (cf. refs [6,11] and Figure 4). For MPDs however, the cation looks slightly softer than the anion (Figure 4). It is interesting to point out that this picture is in agreement with the closeness of the (crystallographic data based) Shannon-Prewitt radii[54,55] for K^+ (138 pm) and F^- (133 pm).

4. Madelung Forces. There is also a feature that can be noticed by a more careful analysis of the data. As a rule, the volume of a given ion X^- (or M^+) increases as the size the counterion M^+ (or X^-) increases. This effect is stronger for (the softer) anions than for the cations and can be seen in Figure 5. An explanation is that as the distance between ions increases when a larger counterion is present, the lattice constant increases, too, and the Madelung

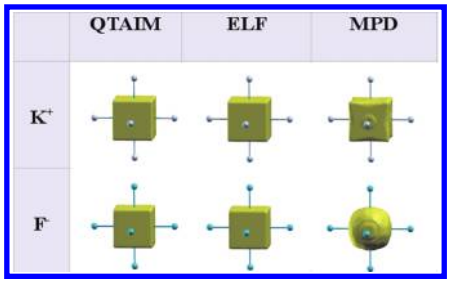

Figure 4. Domains for K^+ (top row) and F^- (bottom row) in KF obtained from QTAIM, ELF, and the MPD (from left to right column).

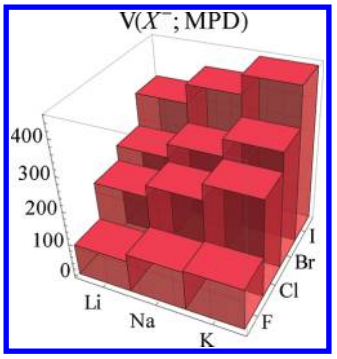

Figure 5. Volume of anionic MPDs, in $bohr^3$.

force decreases. Thus, for larger counterions, the compression of the ion is less important.

5. Space Partitioning. To our numerical accuracy of 1%, we obtain the density or ELF basins partition space. However, up to 5% of the space is missing when adding up the volumes of MPDs. As we find that the average number of electrons for cationic and anionic regions together yields a value close to the correct number of electrons, we interpret the missing part of space as "empty" space. Because an MPD corresponds to an extremum of a probability, any change of the MPD produces changes in the probability that are of second order and makes the "shrinking" of Ω difficult to pinpoint. As we do not have the numerical accuracy yet to analyze it reliably, we would not like to overemphasize this effect.

B. Probabilities. *1. Maximal Probabilities.* Of course, one of the outcomes of the method of MPDs is to provide probability distributions for the electrons in Ω. The maximal probability corresponds to that of having as many electrons as in the free ion. They are quite large, see Figure 6, not only when compared to independent particles, but also when compared, for example, with the probability of finding two particles in the Si−Si bond of the Si crystal ($p_2 \approx 0.4$).[24]

2. p in QTAIM, ELF and MPD. As a consequence of the similitude of the spatial domains, the probability distributions are qualitatively the same for QTAIM or ELF domains, as for the MPDs, compare Figure 7.

This can be explained by realizing that the MPDs maximize the probabilities: changing Ω away from the MPDs only changes p_ν at second order.

3. Electron Surface Crossings. As mentioned above and illustrated in Appendix B, we can expect for most diffuse ions, I^-, the strongest effect of surface crossing (illustrated by the strongest reduction of maximal probability, see Figure 6). The

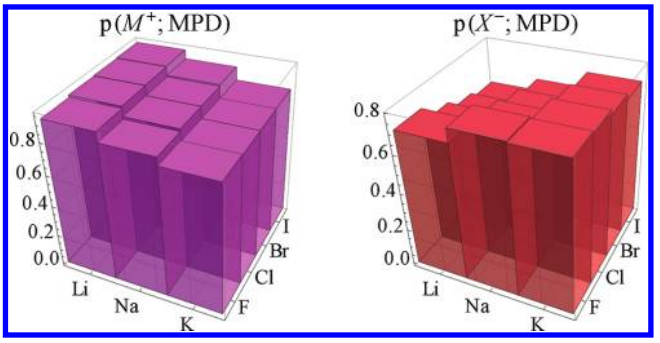

Figure 6. Maximal probabilities, $p_\nu(\Omega_\nu)$, for a domain around a nucleus, containing a number of electrons equal to that of the formal ion (cations M^+, left, and anions X^-, right).

maximal probability decrease is weaker in the cations (from Li to K) than it is in anions.

Surface crossing can be expected to be important when domains have surfaces in contact. Intuitively, one expects that a larger contact surface between anionic domains also favors the penetration effect discussed here. The trend is confirmed by comparing the maximal probabilities for LiI and KI, Figure 6, and the contact surfaces between X^- domains, Figure 3.

Let us now look at the symmetry of probability distributions and their relationship to charges. Wigner-Seitz cells illustrate, by construction, the symmetric case with no charge transfer, and it can be recognized in the symmetric probability distributions (see Figure 7, top). When pseudopotentials are eliminated, and cations are present, the probability distribution for the cationic domains showed an asymmetry (see Figure 7, middle row). By the change in the probabilities (increase of $p_{\nu+1}$ for M^+, and of $p_{\nu-1}$ for X^-), it can be related to a transfer from the ideal ions X^- and M^+, to neutral atoms, X and M. Even when cations are present, the contact surfaces between anionic domains remain important in most cases, and one can still expect an important contribution coming from the symmetric surface crossings. For the anions, we thus find a mixture of the two types of electron surface crossings. The probability distribution in the anions presents an asymmetry toward the neutral atoms. However, it is relatively weak and slightly reduced when going from the QTAIM basins to ELF or MPDs. The dominant effect for anions seems to be the reduction of $p_\nu(\Omega_\nu)$ due to the exchange of electrons between anions, as it was for the Wigner-Seitz cells.

4. Uncommon Ions. As there is a significant probability not only to find X but to also find X^{2-} in the domain attributed to X^-, we would like to ask whether it would be of interest to consider the existence of such charged systems. Of course, they showed up by our construction, by attributing a limited domain of space to the ions, and their probability will probably decrease when correlation is taken into account. But is it not something we should accept as imposed by the quantum description?

If we see this effect as related to a different picture, as due to "penetration" or "overlap", should we replace the concept of "charge" by it? While it is tempting to do it for equivalent domains, should we do it for nonequivalent domains?

5. Charges. In the examples studied in this paper, the deviations from the formal ionic charges are relatively small. The largest deviation observed in the crystals studied, for QTAIM, is ≈0.2. The average deviation from the formal charges is ≈0.1 for QTAIM, and approximately half this value for ELF and MPDs. Notice, however, that these numbers are close to the numerical

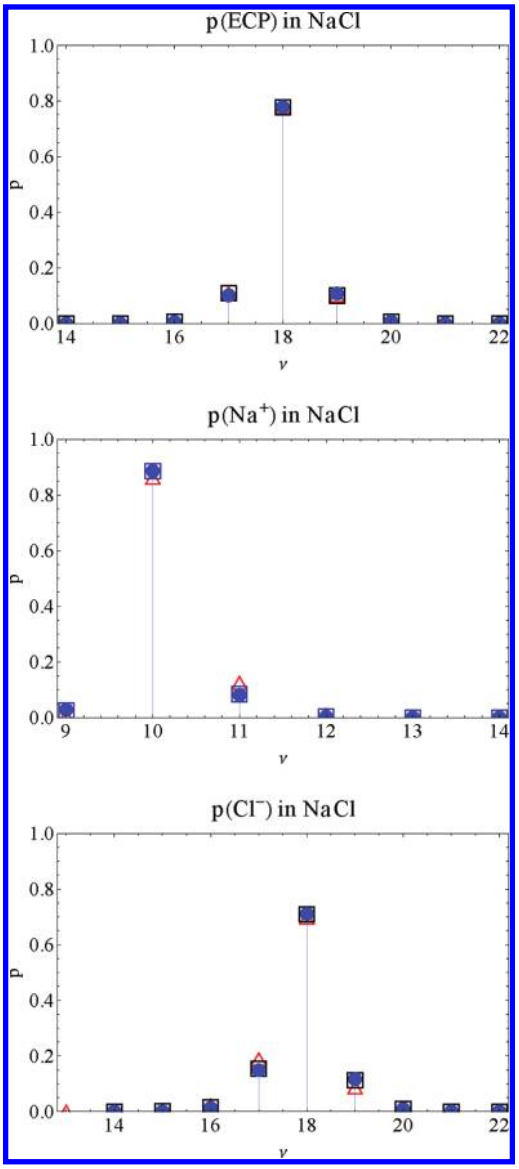

Figure 7. Probability distributions in the NaCl crystal: for a Wigner-Seitz cell of the halogen sublattice, top, for Na^+, middle row, and for Cl^-, bottom. The spatial domains for which the probabilities are computed are the atomic basins of QTAIM, triangles; the MPDs, circles; the domains obtained from ELF, squares, yield probabilities that can be hardly distinguished from the MPD on the scale of this plot.

accuracy of integration of ≈1%. Thus, we can consider that the ionic description is appropriate for the crystals studied here. In view of the precise definitions given for the MPDs, it seems that there is no need to further arguing in favor of the charges obtained, and there is no need to further support the statements made by Bader and Matta[56] in the controversy about the magnitude of the charges.

One might ask what happens if one defines Ωs by choosing ν values corresponding to the number of electrons in the atom and not to that of the ion. We get an "atom" in the crystal, and not an "ion" in the crystal, and can consider its charge, too. We would like to mention first that it has already been noticed before that for physically insignificant domains the maxima are less pronounced and thus more difficult to obtain (cf., Figures 1 and 2 in ref 15). Nevertheless, we have tried to obtain atomic

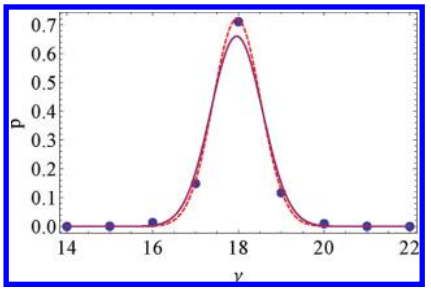

Figure 8. Probability distributions in the NaCl crystal, dots; a Gaussian function having the same mean and variance as the distribution, full curve; a Gaussian function fitting this distribution, dashed curve.

domains for the NaCl crystal and found that the changes are dramatic.

1. The Na atomic domain is much larger than that of the ionic domain; the reverse occurs for Cl.
2. The probabilities to find as many electrons as in the atom (≈0.4) are approximately half those obtained for the finding in the ionic domain as many electrons as in the free ion.
3. The atomic domains bear (on average) almost no charge, but there is a significant probability to find ionic structures, ≈0.3 for the expected ions Na^+ and Cl^- and ≈0.2 for the unexpected ions Na^- and Cl^+.

Thus, one does not reach the same conclusion about the degree of ionicity, starting with the "atom" in the crystal as with the "ion" in the crystal.

Thus, in spite of being able to obtain charges and even define them rigorously, we believe that one must be very careful in using them. We would like to sustain our statement with charges, obtained from measurable data, namely, dipole moments, equilibrium distances, and derivatives of the dipole moment wrt the distance. It turns out that the charges obtained cannot even be kept for the zero-point vibration (see Appendix C). For the present paper, we do not want to continue with this type of questioning and simply stay with the data we have produced, the probability distributions in the Ωs.

6. Reducing the Probability Distribution to Mean and Variance. Although the mean (eq 2) and the variance (eq 5) provide important information about the probability distribution, we would like to illustrate that this may not be sufficient to reconstruct it. To do it, let us assume that we can safely neglect all probabilities except those for $\nu - 1$, ν, and $\nu + 1$. This seems to be well justified by the plots in Figure 8. Knowing also that the probabilities have to sum to 1, we can try to use the mean, eq 2, and variance, eq 5, to determine the three important probabilities. To make the argument quantitative, we define $\delta = p(\nu + 1) - p(\nu - 1)$ as a measure of the asymmetry of the probability distribution. One obtains for the mean $\mu = \nu + \delta$. Thus, at no surprise, $\mu - \nu$ is a good measure for the asymmetry of the probability distribution. For the variance, one obtains $\sigma^2 = 1 - p(\nu) - \delta^2$. We see that the last term can be neglected, when δ is small, and that the variance indicates the decrease of $p(\nu)$ from the maximal value of one. It turns out, however, that, in spite of the smallness of the probabilities neglected, the error propagation can be significant. For example, from the probability distribution obtained for the domain optimized for Cl^- in NaCl, one can compute $\mu \approx 17.96$ and $\sigma^2 \approx 0.37$. One can now use this information to obtain backward $p_{\nu-1=17}$, $p_{\nu=18}$, and $p_{\nu+1=19}$. While δ is reproduced reasonably well (−0.03 instead of −0.04), p_ν is

underestimated (0.63 instead of 0.71). This is understandable: the probabilities for finding a number of electrons largely different from $\nu - 1$, ν, or $\nu + 1$ are small, but they are more heavily weighted in the variance. A fit to Gaussian distribution[57,58] can sustain this point making the discrete points of the exact probability distribution lie quite close to the fit,[53] which, however, has a different variance ($\approx$0.30).

VI. CONCLUSIONS

This paper presents a new program that (i) computes the probabilities to find a given number of electrons in a spatial domain within a crystal and (ii) optimizes this domain to maximize the probability of finding a chosen number of electrons; the domain obtained is a maximum probability domain (MPD). The program is used to analyze crystals studied in the rock-salt structure (MX; M: Li, Na, K; X: F, Cl, Br, I), where a physical intuition suggests a strong ionic character. We produced spatial domains for which the probability to find the same number of electrons as in a free ion is maximal.

For all systems studied, the MPDs resemble the atomic basins of QTAIM or collections of ELF basins. This might be less surprising for ELF basins, as, for single Slater determinants, in the ideal limiting case of strictly localized (nonoverlapping) orbitals, the localization domain of the orbitals, the ELF basins, and the MPDs become identical.[59] The similitude with QTAIM density basins probably stems from the remains of an atomic shell structure, which is reproduced by all three methods. This similitude is an effect specific to the systems studied in this paper and not a general feature: (i) in the Si crystal, the density basins differ qualitatively from those produced by ELF basins and MPDs, compare ref 24; (ii) in the bent Si_2H_2, the ELF basins are also different from the MPDs.[12]

The resulting picture is in accord with the conventional one, the MX crystals being predominantly ionic, in the sense that the probability of finding an number of electrons equal to that of a free ion is relatively large. Of course, fluctuations are unavoidable.

We interpret the trends in probability changes using other physical concepts like compactness of the ions, contact surfaces between ions, distance between them and Madelung forces.

Finally, we mention some side issues of this paper. One is to point out that using synthetic quantities like mean (or population or charge) and variance might not be enough to correctly characterize the probability distribution. We also discuss the definition of the charge. Usually the charge is related to populations (to the mean of the probability distribution). However, probability distributions can show a non-negligible probability of finding a number of electrons different from the formal one. We naturally find charge fluctuations between ions of different kind, which can be asymmetric and induce net charges, but fluctuations can also be symmetric, as between ions of the same kind, and increase the probability of finding a differently charged system.

We knowingly did not address the issue of transferability, and hint to the difficulty of enterprising it by illustrating it in an appendix by showing that two different, well-defined, measurable "charges", can be qualitatively different. We also found it useful to clarify the interpretation of electron density, also in an appendix.

APPENDIX A: PHYSICAL SIGNIFICANCE OF THE ELECTRON DENSITY

Usually $\rho(r)$ times the volume element is interpreted as the probability to find an electron in the volume element around r. However, this produces the paradox that the integral over all space yields the total number of electrons, N, which, in general, is larger than 1, the upper limit for a probability. Sometimes, it is argued that the density should be normalized to 1, and not to N, in order to be a probability. The solution to this paradox is simple. The density, normalized to N, integrated over the volume yields not the probability mentioned, but the average number of electrons in it, compare equations 3 and 4. When the volume becomes very small, (i) the integral becomes $\rho(r)$ times the volume element and (ii) the probability of finding more than one electron vanishes. Thus, the average number of electrons for a vanishingly small Ω becomes the probability to find one electron in it

$$\rho(r)V_\Omega \approx \int_\Omega \rho(r)\mathrm{d}^3r = \langle\Psi|\hat{N}_\Omega|\Psi\rangle \approx 0p_0(\Omega) + 1p_1(\Omega) + \ldots = p_1(\Omega) + \ldots \quad \text{(A1)}$$

where V_Ω is the volume of the Ω.

APPENDIX B: TWO CLOSED-SHELL ATOMS MODEL

To better understand surface crossings by electrons, let us consider a simple two-center model, described by a hydrogenic orbital (with exponent ζ) on each of the center. Two of the electrons occupy the σ_g orbital, two more the σ_u orbital. In a localized picture, we have two closed shells, compact if ζ is large, diffuse if ζ is small. The centers are at distance R. A plane perpendicular to the internuclear axis, equally distant from the two nuclei, produces two equivalent half-spaces. The probabilities to find ν electrons in one of the half-spaces can be computed analytically and depend on ζR. When $\zeta R \rightarrow \infty$, we are certain that two and only two electrons are in the half-space: $p_2 \rightarrow 1$. In this case, the two subsystems are well separated, either by being compact, or by their distance. While p_2 decreases monotonically with ζR, $p_1 = p_3$ increase, and $p_0 = p_4 \approx 0$ are almost unchanged. Thus, there is a finite probability not to have two electrons for a finite separation between the two closed shell "atoms". The origin of this is that the plane splitting the space in two halves can be crossed by the electrons (the hydrogenic wave function crosses it more and more as ζR decreases). From this model we expect that for more diffuse systems (smaller ζ) this penetration effect (or electron surface crossing, or fluctuation) is more important than for more compact systems. However, more diffuse systems may also be associated to larger distances between nuclei, and thus the opposite effect (increased R) may also happen.

APPENDIX C: "EXPERIMENTAL" CHARGES

Let us try to define "charges" in the first-row diatomic hydrides LiH, BeH, BH, ..., HF, using only measurable quantities. If atomic charges could be associated to atomic centers, one could obtain a "static" charge, from the values of the dipole moments, m, divided by the bond length, R:

$$q_{\text{static}} = m/R \quad \text{(C1)}$$

Alternatively, one could define a "dynamic" charge, as the derivative of the dipole moment with respect to the bond

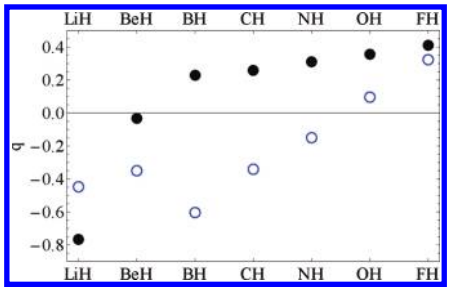

Figure 9. Charges in first row hydrides defined as the ratio of dipole moments to internuclear distances, filled circles, and as derivatives of the dipole moment wrt the internuclear distance, empty circles.

length, R:

$$q_{\text{dynamic}} = \frac{dm}{dR} \tag{C2}$$

Although one might use experimental data for these charges, we use here, for consistency, the calculated data (CEPA) of ref 60. Figure 9 shows important differences between the two definitions. For BH, CH, and NH, not even the sign of the charge is the same for the two definitions. This should not be too surprising. It has been known for a long time that changing the bond length also induces changes in the charge distribution (see, e.g., ref 61 or, for a more recent application, ref 62). The static charge, q_{static}, is qualitatively different from that arising from infinitesimal changes in the bond length. Please notice that centering the charges in points away for the nuclei does not change the sign and, thus, will not correct the discrepancy for BH, CH, or NH.

■ ASSOCIATED CONTENT

Ⓢ Supporting Information. Raw numerical data used in the discussion. This material is available free of charge via the Internet at http://pubs.acs.org.

■ AUTHOR INFORMATION

Corresponding Author

*E-mail: mauro.causa@unina.it; andreas.savin@lct.jussieu.fr.

■ REFERENCES

(1) Bader, R. F. W. *Atoms in Molecules: A Quantum Theory*; Oxford University Press: Oxford, 1990.
(2) Becke, A.; Edgecombe, K. E. *J. Chem. Phys.* **1990**, *92*, 5397.
(3) Savin, A. In *Reviews of Modern Quantum Chemistry: A Celebration of the Contributions of Robert G. Parr*; Sen, K. D., Ed.; World Scientific: Singapore, 2002; p 43.
(4) Kohout, M.; Wagner, F. R.; Grin, Y. *Intern. J. Quantum Chem.* **2006**, *106*, 1499.
(5) Martín Pendás, A.; Costales, A.; Luaña, V. *Phys. Rev. B* **1997**, *55*, 4275.
(6) Martín Pendás, A.; Costales, A.; Luaña, V. *J. Phys. Chem. B* **1998**, *102*, 6937.
(7) Kohout, M. Dissertation, Universität Stuttgart, Germany, 1999.
(8) Blanco, M. A.; Costales, A.; Martín Pendás, A.; Luaña, V. *Phys. Rev. B* **2000**, *68*, 12028.
(9) Martín Pendás, A.; Costales, A.; Blanco, M.; Recio, J. M.; Luaña, V. *Phys. Rev. B* **2000**, *62*, 13970.
(10) Baranov, A.; Kohout, M.; Wagner, F. R.; Grin, Y.; Kniep, R.; Bronger, W. *Z. Anorg. Allg. Chem.* **2008**, *634*, 2747.
(11) Baranov, A. I.; Kohout, M. *J. Comput. Chem.* **2011**, *32*, 2064.
(12) Scemama, A.; Caffarel, M.; Savin, A. *J. Comput. Chem.* **2007**, *28*, 442.
(13) Claverie, P.; Diner, S. In *Localization and Delocalization in Quantum Chemistry*; Chalvet, O., Daudel, R., Diner, S., Malrieu, J., Eds.; D. Reidel: Dordrecht, 1976; Vol. 2, p 395.
(14) Cohen-Tannoudji, C.; Diu, B.; Laloe, F. *Mécanique Quantique*; Hermann: Paris, 1977.
(15) Cancès, E.; Keriven, R.; Lodier, F.; Savin, A. *Theor. Chem. Acc.* **2004**, *111*, 373.
(16) Bader, R. F. W.; Stephens, M. E. *Chem. Phys. Lett.* **1974**, *26*, 445.
(17) Bader, R. F. W.; Stephens, M. E. *J. Am. Chem. Soc.* **1975**, *97*, 7391.
(18) Savin, A.; Silvi, B.; Colonna, F. *Can. J. Chem.* **1996**, *74*, 1088.
(19) Chamorro, E.; Fuentealba, P.; Savin, A. *J. Comput. Chem.* **2003**, *24*, 496.
(20) Silvi, B.; Savin, A. *Nature* **1994**, *371*, 683.
(21) Kohout, M.; Wagner, F. R.; Grin, Y. *Theor. Chem. Acc.* **2002**, *108*, 150.
(22) Silvi, B. *J. Mol. Struct.* **2002**, *610*, 277.
(23) Mafra Lopes, O., Braïda, B., Causà, M., Savin, A., Hoggan, P., et al., Eds. Advances in the Theory of Quantum Systems in Chemistry and Physics. *Progress in Theoretical Chemistry and Physics*; Springer: Berlin, 2011; Vol. 22, page xx.
(24) Causà, M.; Savin, A. *Z. Anorg. Allg. Chem.* **2011**, *637*, doi: 10.1002/zaac.201100156.
(25) Daudel, R. *C. R. Acad. Sci. Fr.* **1953**, *237*, 691.
(26) Daudel, R.; Brion, H.; Odiot, S. *J. Chem. Phys.* **1955**, *23*, 2080.
(27) Aslangul, C.; Constanciel, R.; Daudel, R.; Kottis, P. *Adv. Quantum Chem.* **1972**, *6*, 93.
(28) Francisco, E.; Martín Pendás, A.; Blanco, A. M. *J. Chem. Phys.* **2007**, *126* (9), 094102.
(29) Francisco, E.; Martín Pendás, A.; Blanco, M. A. *Comput. Phys. Commun.* **2008**, *178*, 621.
(30) Scemama, A. *J. Theor. Comp. Chem.* **2005**, *4*, 397.
(31) Boys, S. F.; Rajagopal, P. *Adv. Quantum Chem.* **1965**, *2*, 1.
(32) Becke, A. D. *J. Chem. Phys.* **1988**, *88*, 2547.
(33) Towler, M. D.; Zupan, A.; Causà, M. *Comput. Phys. Commun.* **1996**, *98*, 181.
(34) Causà, M. In *Quantum-Mechanical Ab Initio Calculation of the Properties of Crystalline Materials, Lecture Notes in Chemistry*; Pisani, C., Ed.; Springer-Verlag: Berlin, 1996; Vol. 67, p 91.
(35) Zicovich-Wilson, C.; Dovesi, R.; Saunders, V. *J. Chem. Phys.* **2001**, *115*, 9708.
(36) Dovesi, R.; Orlando, R.; Civalleri, B.; Roetti, C.; Saunders, V. R.; Zicovich-Wilson, C. M. *Z. Kristallogr.* **2005**, *220*, 571.
(37) Saunders, V. R.; Dovesi, R.; Roetti, C.; Causà, M.; Harrison, N. M.; Orlando, R.; Zicovich-Wilson, C. M. *CRYSTAL98*, CRYSTAL98 User's Manual; University of Torino: Torino, 1998.
(38) Dovesi, R.; Saunders, V. R.; Roetti, C.; Orlando, R.; Zicovich-Wilson, C. M.; Pascale, F.; Civalleri, B.; Doll, K.; Harrison, N. M.; Bush, I. J.; DArco, P.; Llunells, M. *CRYSTAL98*, CRYSTAL98 User's Manual; University of Torino: Torino, 2009.
(39) www.crystal.unito.it.
(40) Wycoff, R. W. G. *Crystal Structures*; John Wiley & Sons: London, 1963; Vol. 1.
(41) Wycoff, R. W. G. *Crystal Structures*; John Wiley & Sons: London, 1964; Vol. 2.
(42) http://www.theochem.uni-stuttgart.de/pseudopotentials.
(43) Peterson, K.; Figgen, D.; Goll, E.; Stoll, H.; Dolg, M. *J. Chem. Phys.* **2003**, *119*, 11113.
(44) Peterson, K.; Shepler, B.; Figgen, D.; Stoll, H. *J. Phys. Chem. A* **2006**, *110*, 13877.
(45) Fuentealba, P.; Preuss, H.; Stoll, H.; v. Szentpaly, L. *Chem. Phys. Lett.* **1982**, *89*, 418.
(46) Ojamäe, L.; Hermansson, K.; Pisani, C.; Causà, M. *Acta Crystallogr., Sect. B* **1994**, *50*, 268.

(47) Dovesi, R.; Roetti, C.; Freyria Fava, C.; Prencipe, M.; Saunders, V. R. *Chem. Phys.* **1991**, *156*, 11.
(48) Civalleri, B.; Ferrari, A.; Llunell, M.; Orlando, R.; Merawa, M.; Ugliengo, P. *Chem. Mater.* **2003**, *15*, 3996.
(49) Nada, R.; Catlow, C.; Pisani, C.; Orlando, R. *Model. Simul. Mater. Sci. Eng.* **1993**, *1*, 165.
(50) Aprà, E.; Causà, M.; Prencipe, M.; Dovesi, R.; Saunders, V. *J. Phys.: Condens. Matter* **1993**, *5*, 2969.
(51) Kokalj, A.; Causà, M. Proceedings of High Performance Graphics Systems and Applications European Workshop, Bologna, Italy, 2000; p 51.
(52) Kokalj, A. *Comput. Mater. Sci.* **2003**, *28*, 155.
(53) Wolfram, S. *Mathematica ed.*, Version 7.0; Wolfram Research, Inc: Champaign, IL, 2008.
(54) Shannon, R. *Acta Crystallogr., Sect. A* **1976**, *32*, 751.
(55) Shannon, R.; Prewitt, C. T. *Acta Crystallogr., Sect. B* **1969**, *25*, 925.
(56) Bader, R. F. W.; Matta, C. F. *J. Phys. Chem. A* **2004**, *108*, 8385.
(57) Pfirsch, F.; Böhm, M. C.; Fulde, P. *Z. Phys. B* **1985**, *60*, 171.
(58) Fulde, P. *Electron Correlations in Molecules and Solids*; Springer: Berlin, 1991.
(59) Savin, A. *J. Chem. Sci.* **2005**, *117*, 473.
(60) Meyer, W.; Rosmus, P. *J. Chem. Phys.* **1975**, *63*, 2356.
(61) Rittner, E. S. *J. Chem. Phys.* **1951**, *19*, 1030.
(62) Pauzat, F.; Pilmé, J.; Toulouse, J.; Ellinger, Y. *J. Chem. Phys.* **2010**, *133*, 054301.